

Gate-tunable giant superconducting nonreciprocal transport in few-layer T_d -MoTe₂

T. Wakamura,¹ M. Hashisaka,¹ S. Hoshino², M. Bard¹, S. Okazaki,³ T. Sasagawa,³ T. Taniguchi,⁴ K. Watanabe,⁵ K. Muraki,¹ and N. Kumada¹

¹*NTT Basic Research Laboratories, NTT Corporation, 3-1 Morinosato-Wakamiya, Atsugi, 243-0198, Japan*

²*Department of Physics, Saitama University, Shimo-Okubo, Saitama 338-8570, Japan*

³*Laboratory for Materials and Structures, Tokyo Institute of Technology, Nagatsuta, 226-8503, Japan*

⁴*International Center for Materials Nanoarchitectonics,*

National Institute for Materials and Science, 1-1 Namiki, Tsukuba, 305-0044, Japan and

⁵*Research Center for Functional Materials, National Institute for Materials and Science, 1-1 Namiki, Tsukuba, 305-0044, Japan*
(Dated: March 20, 2023)

We demonstrate gate-tunable giant field-dependent nonreciprocal transport (magneto-chiral anisotropy) in a noncentrosymmetric superconductor T_d -MoTe₂ in the thin limit. Giant magneto-chiral anisotropy (MCA) with a rectification coefficient $\gamma = 3.1 \times 10^6 \text{ T}^{-1} \text{ A}^{-1}$, is observed at 230 mK, below the superconducting transition temperature (T_c). This is one of the largest values reported so far and is likely attributed to the reduced symmetry of the crystal structure. The temperature dependence of γ indicates that the ratchet-like motion of magnetic vortices is the origin of the MCA, as supported by our theoretical model. For bilayer T_d -MoTe₂, we successfully perform gate control of the MCA and realize threefold modulation of γ . Our experimental results provide a new route to realizing electrically controllable superconducting rectification devices in a single material.

Recent intensive studies on nonreciprocal transport have revealed the potential of using noncentrosymmetric materials or inversion-symmetry-breaking multilayer structures to develop novel rectification devices [1–3]. In systems with broken inversion and time-reversal symmetries, Onsager’s reciprocal theorem allows the electrical resistance to be different for opposite current directions. This is called magneto-chiral anisotropy (MCA), and it leads to the rectification effect [1].

Broken inversion symmetry is more profitable in superconductors. Rectification via ratchet-like motion of magnetic vortices was reported more than a decade ago for superconductors with asymmetric artificial magnetic nanostructures or with asymmetric antidots as an asymmetric pinning potential, and it was found that as the asymmetry becomes stronger, rectification is more efficient [4–9]. Recent studies have pointed out that such ratchet-like motion of magnetic vortices is also possible in noncentrosymmetric superconductors and provides large MCA as for other mechanisms such as paraconductivity [10–14]. In such systems, the asymmetry of the crystal structure intrinsically induces asymmetric pinning potential for magnetic vortices. Taking the analogy with previous findings on superconductors with artificial asymmetric pinning potentials, the symmetry of the crystal should play a crucial role for the efficiency of the rectification. However, previous reports on MCA in noncentrosymmetric superconductors has been limited to those with trigonal symmetry [11, 12, 15–17]. Therefore, it is particularly called for to explore MCA in noncentrosymmetric superconductors with different symmetries, especially with lower symmetry than trigonal symmetry for further enhancement of the efficiency.

In this Letter, we demonstrate gate-tunable giant MCA in a noncentrosymmetric superconductor T_d -

MoTe₂ in the thin limit. T_d -MoTe₂ lacks inversion symmetry and, for thin layers, has only one mirror plane normal to the b -axis as shown in Fig. 1(a). This reduced symmetry of the crystal structure may make the pinning potential for magnetic vortices highly asymmetric, which can generate a large MCA. We exploit few-layer

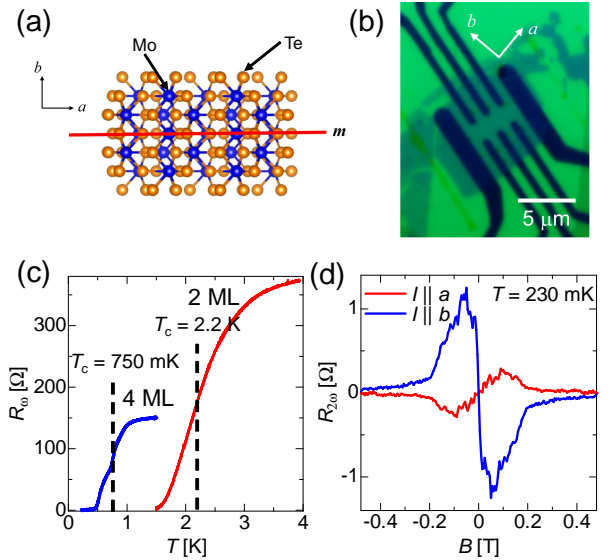


FIG. 1. (a) Top view of the crystal structure, in which broken inversion symmetry is evident. For thin layers, only one mirror plane is present. (b) Optical microscope image of a 4 ML device. A thin T_d -MoTe₂ flake is deposited on metallic contacts prepared in advance. (c) Temperature dependence of the resistance of 4 ML and bilayer samples. (d) Comparison of $R_{2\omega}$ when current is parallel to the a -axis (red) and b -axis (blue) taken of the 4 ML sample.

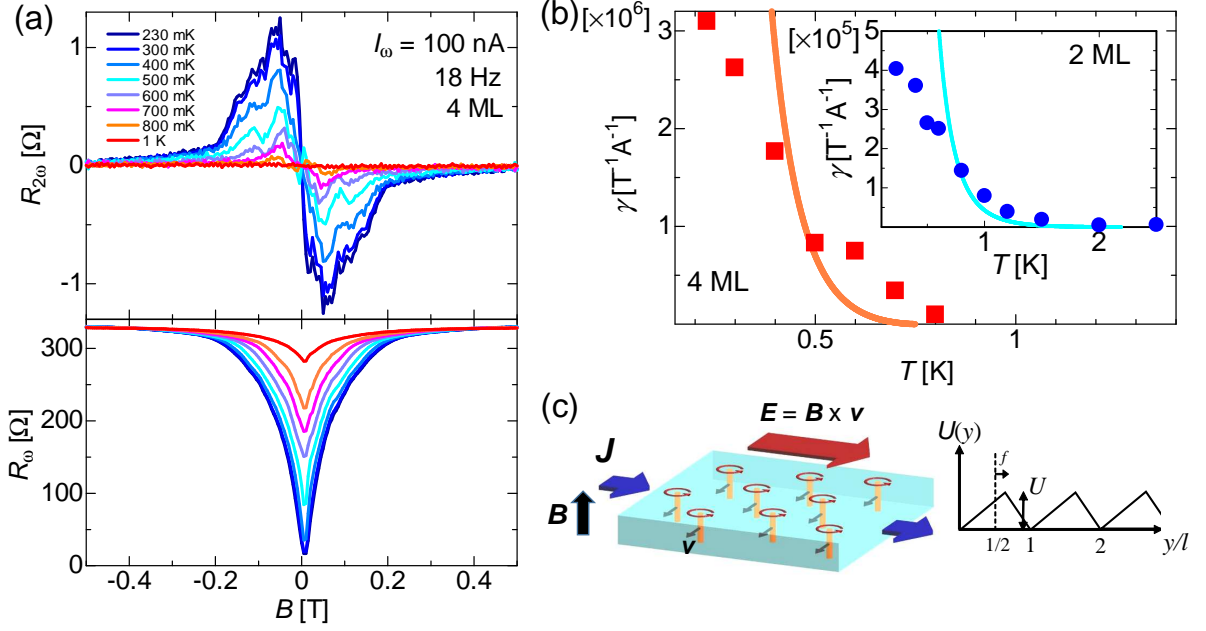


FIG. 2. (a) Experimental data from the 4 ML sample. Top: Nonreciprocal resistance ($R_{2\omega} = V_{2\omega}/I_{\omega}$) measured at different temperatures. Bottom: R_{ω} signals measured simultaneously with $R_{2\omega}$. (b) Temperature dependence of γ taken from the 4 ML sample. The orange curve shows the fit based on equation (3). Inset: Experimental data of γ as a function of temperature obtained from the bilayer sample with the fit. (c) Left: Schematic illustration of the motion of magnetic vortices with the velocity \mathbf{v} driven by an external current \mathbf{J} , which generates an electric field $\mathbf{E} = \mathbf{B} \times \mathbf{v}$. Right: Image of sawtooth potential assumed as the ratchet pinning potential in (3).

T_d -MoTe₂ for our measurements. Below T_c , we observe MCA under a perpendicular magnetic field. The rectification coefficient γ , i.e., the ratio of the nonreciprocal (second harmonic) resistance to the linear resistance, reaches $3.1 \times 10^6 \text{ T}^{-1}\text{A}^{-1}$ at 230 mK, one of the largest values reported so far. The monotonic increase in γ with decreasing temperature indicates that the giant MCA is due to the ratchet-like motion of magnetic vortices in the mixed state of the type-II superconductor [10]. Interestingly, despite that T_d -MoTe₂ is a semimetal, in the bilayer sample we can successfully modulate the MCA via an external gate voltage and demonstrate threefold modulation of γ . This ability to produce a large variation in the nonreciprocal resistance by changing the gate voltage may provide key insights into the mechanisms behind the giant MCA by associating it with modulation of the superconducting properties.

Thin semimetallic MoTe₂ samples are prepared from high-quality T_d -MoTe₂ crystals with a residual-resistivity ratio (RRR) ~ 1000 grown via the flux growth method. Mechanically exfoliated flakes are transferred onto prepatterned electrodes on a Si/SiO₂ chip or hexagonal boron-nitride (h-BN) deposited on a Si/SiO₂ chip by a typical dry transfer technique with polycarbonate (PC) and polydimethylpolysiloxane (PDMS) [18] in an argon-filled glovebox with a low concentration of O₂ and H₂O (< 0.5 ppm). Electrical measurements are performed with a lock-in amplifier and ³He low temperature mea-

surement system. More details of the fabrication process and measurement setup are in the Supplemental Material [19].

In materials under broken inversion and time-reversal symmetries, Onsager's reciprocal theorem allows the linear longitudinal resistance to be different for opposite current directions [1]. Rikken *et al.* heuristically found a general formula for the nonreciprocal transport, also called the MCA, expressed as [20]

$$R = R_0(1 + \gamma BI), \quad (1)$$

where γ is the rectification coefficient, which quantifies the efficiency of generating the nonreciprocal resistance. R_0 , B and I are the linear resistance, magnetic field and excitation current, respectively. Substituting equation (1) into Ohm's law $V = RI$ leads to

$$V = R_0 I + \gamma B R_0 I^2. \quad (2)$$

The first term is the typical linear voltage response to the current and the second term is related to the nonreciprocal transport. Thus, the nonreciprocal response is obtained as a second harmonic signal for the ac excitation current $I_{\omega} \propto \sin(\omega t)$.

First, we show the temperature dependence of the resistance for the four monolayer (ML) and bilayer (2 ML) samples in Fig. 1(c). While T_c is low (~ 100 mK) for bulk T_d -MoTe₂ [21], that for the 4 ML and bilayer samples is

750 mK and 2.2 K, respectively. This large enhancement in T_c for thin layers is consistent with previous studies [22, 23]. Note that here T_c is defined as the temperature where the resistance becomes half of that in the normal state.

Now let us focus on measuring the nonreciprocal transport in the superconducting state. Figure 1(d) shows the second-harmonic longitudinal resistance $R_{2\omega}$ for $I_\omega \parallel b$ and for $I_\omega \parallel a$ at 230 mK. a and b are the crystal axes as defined in Fig. 1(a). A clear peak and dip are observed in $R_{2\omega}$ for $I_\omega \parallel b$. The field-asymmetric $R_{2\omega}$ signals are in agreement with the MCA in (1) and are consistent with previous experimental results [11, 15, 16, 24]. Note that the nonlinearity of the resistance due to the transition between the normal and superconducting state is symmetric in B , so it is excluded as the origin of $R_{2\omega}$. In contrast to the case for $I_\omega \parallel b$, $R_{2\omega}$ for $I_\omega \parallel a$ is dramatically suppressed. This is also consistent with the geometry of MCA, where the symmetry plane, the directions of the magnetic field and generated second-harmonic voltage are all perpendicular to each other [1]. Note that the finite signal for $I_\omega \parallel a$ is due to misalignment of the electrodes to the crystal axis (see Fig. 1(b)) [19]. Below we focus on the geometry where $I_\omega \parallel b$.

The top part of Fig. 2(a) displays $R_{2\omega}$ as a function of perpendicular magnetic field measured at different temperatures. The amplitude of the signals monotonically decreases with increasing temperature. Above T_c , $R_{2\omega}$ is completely suppressed, indicating that the effect is related to superconductivity. The bottom part of Fig. 2(a) displays the R_ω signals measured simultaneously with the $R_{2\omega}$ signals.

Now that we have obtained $R_{2\omega}$ and R_ω , we can estimate the value of the rectification coefficient $\gamma = 2R_{2\omega}/(R_\omega BI_\omega)$ [1, 10, 15]. To obtain γ , we use the values of R_ω and $R_{2\omega}$ at B where $R_{2\omega}$ is at a peak. Figure 2(b) shows that γ continues to increase with decreasing temperature and reaches $\gamma = 3.1 \times 10^6 \text{ T}^{-1} \text{ A}^{-1}$ at 230 mK, the lowest measurement temperature. This value is two to three orders of magnitude larger than that of other two-dimensional superconductors, such as MoS₂ and NbSe₂ as we will discuss later. In the inset of Fig. 2(b) we also plot the temperature dependence of γ for the bilayer sample, which shows the similar trend with slightly smaller amplitudes than those of the 4 ML sample.

So far, several mechanisms have been proposed to explain the MCA in the superconducting state [10, 14]. The temperature dependence of the signals and the direction of the applied magnetic field are clues with which to determine the mechanism. For example, paraconductivity is one of the mechanisms proposed as an origin of MCA under an in-plane magnetic field. Since it is relevant to thermal fluctuations of the superconducting order parameter, the nonreciprocal signal is slightly enhanced above T_c and suppressed much below T_c . On the other hand, the ratchet-like motion of the magnetic vortices enhances the MCA below T_c under a perpendicular mag-

netic field [10]. In the mixed state of type-II superconductors, magnetic fluxes penetrate the superconductor, and they are usually trapped by pinning potentials induced by disorder. External current can drive the magnetic fluxes through the Lorenz force as schematically shown in the left image of Fig. 2(c), if it is large enough to overcome the pinning potential [25, 26]. In superconductors with broken inversion symmetry, the asymmetry of the crystal structure locally affects the shape of the pinning potentials, making them asymmetric [20, 27]. In this case, the magnetic vortices can exhibit ratchet-like motion, where the leftward and rightward motion of the vortex is not equivalent [4, 5]. This asymmetry provides a source for nonreciprocal transport [4–8, 10–12, 16]. Increasing γ with decreasing temperature is consistent with the ratchet-like motion of the magnetic vortices as the origin of the MCA [10]. Such a temperature dependence is because thermal fluctuations of the magnetic vortices inside the pinning potential, which disturb the ratchet motion, are suppressed with decreasing temperature, and also the coherence length, which determines the diameter of the vortex, becomes smaller, making the vortex more sensitive to the pinning potentials.

In Fig. 2(b), we plot the theoretical fit to the experimental data based on the following theoretical expression assuming the ratchet-like motion of magnetic vortices as the origin of the MCA [10, 17, 19]:

$$\gamma = \frac{\phi_0^* \beta \ell}{WB} \frac{g_2(\beta U)}{g_1(\beta U)}, \quad (3)$$

where W is the width of the sample, $\phi_0^* = h/2|e|$ is the flux quantum and $\beta = 1/k_B T$ is the inverse temperature. ℓ and U are the mean periodicity and the height of the pinning potential for a vortex, respectively. We take the simple potential shape shown in the right figure of Fig. 2(c), where the dimensionless parameter f controls the asymmetry of the potential. g_1 and g_2 are dimensionless functions determined from the linear- and second-order responses. The ratio is given by $\frac{g_2(\beta U)}{g_1(\beta U)} \sim \frac{f(\beta U)^3}{180}$ for a moving vortex regime with a small ratchet potential. The fits follow the experimental data qualitatively as shown in Fig. 2(b), which supports the ratchet-like motion of magnetic vortices as the dominant mechanism for the giant MCA in this system. There are two fitting parameters, and we emphasize that the fits shown in Fig. 2(b) are obtained by using the same fitting parameters both for the 4 ML and bilayer sample, which also corroborates the validity of our theoretical model (see SM for more details [19]). Note that the vortex picture may be justified specifically in the intermediate temperature range below T_c . At higher temperatures, the vortex mechanism should be replaced by superconducting fluctuation and normal contributions [15]. The origin of the deviation at lower temperatures can be explained by quantum effects of the ratchet-like motion of vortices [28], where quantum tunneling through the ratchet potential suppresses the MCA [11]. Nonetheless, the monotonic enhancement of γ with decreasing temper-

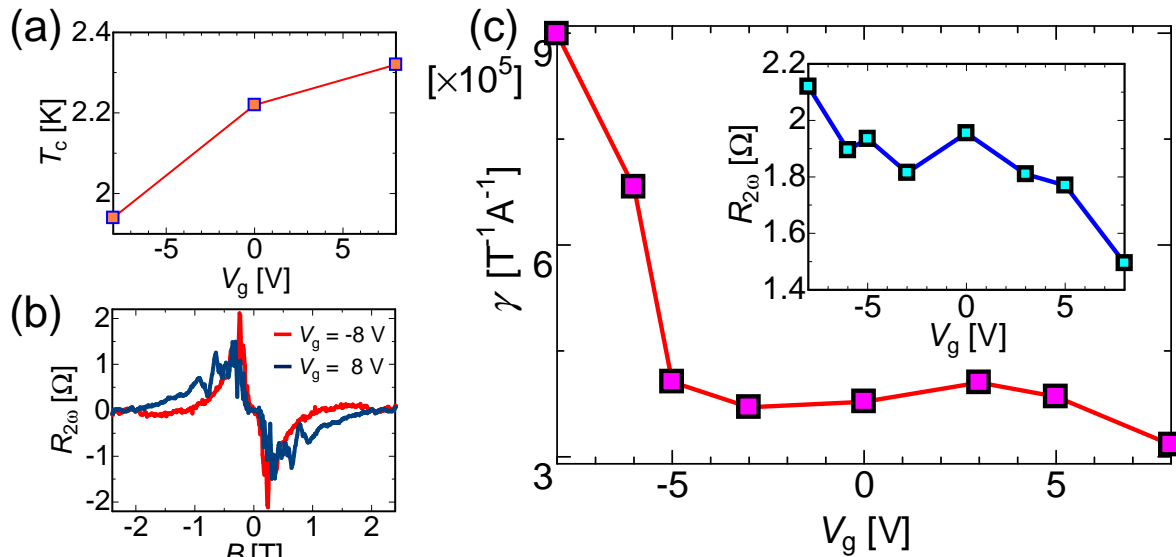


FIG. 3. (a) Gate voltage (V_g) dependence of T_c for the bilayer sample taken at 230 mK. (b) $R_{2\omega}$ as a function of B at different V_g at 230 mK. (c) γ as a function of V_g . Inset: Gate voltage dependence of $R_{2\omega}$.

ature represents the advantage of T_d -MoTe₂ compared to other high- γ noncentrosymmetric superconductors with paraconductivity-based nonreciprocal transport, because even larger γ is expected at lower temperatures, and the temperature range for large γ is much broader [24].

We next discuss the amplitude of γ . Superconductors with trigonal symmetry are often used in MCA measurements, and $\gamma = 8.0 \times 10^3 \text{ T}^{-1} \text{ A}^{-1}$ and $3.4 \times 10^4 \text{ T}^{-1} \text{ A}^{-1}$ have been obtained for MoS₂ and NbSe₂, respectively [15, 16]. These values are two or three orders of magnitude smaller than the value of $\gamma = 3.1 \times 10^6 \text{ T}^{-1} \text{ A}^{-1}$ obtained in our study. The only value comparable to ours reported in the previous studies is $\gamma = 3.2 \times 10^6 \text{ T}^{-1} \text{ A}^{-1}$ from a SrTiO₃ Rashba superconductor under an in-plane magnetic field [24]. As for nonsuperconducting material with broken inversion symmetry, (Bi_{1-x}Sb_x)₂Te₃ (BST) topological nanowires provide $\gamma \sim 1.0 \times 10^5 \text{ T}^{-1} \text{ A}^{-1}$ [3]. Therefore, the value obtained in our study is one of the largest reported so far [11, 12, 15–17]. We attribute this gigantic enhancement in γ to the reduced symmetry of T_d -MoTe₂ compared with other noncentrosymmetric superconductors employed in the previous studies. In comparison with other two-dimensional superconductors with trigonal symmetry, T_d -MoTe₂ has reduced symmetry with only one mirror plane for thin layers. This reduced symmetry affects the asymmetry of the pinning potential. Since the symmetry of the pinning potential is crucial for the vortex dynamics, as reported previously [8, 9, 29, 30], the lower symmetry in the pinning potentials may generate larger nonreciprocal signals.

Finally, we demonstrate the gate modulation of the MCA for the bilayer T_d -MoTe₂. While gate control of the MCA in the normal state has been studied in a BST topo-

logical nanowire [3] and at the LaTiO₃/SrTiO₃ interface [31], it has not been reported yet in superconductors. The primary reason for this is that the concentration of charge carriers in a superconductor is typically high, making it challenging to employ a conventional solid gate to regulate superconducting characteristics due to the electric field screening on the nanometer scale within the material. We can overcome this problem by thinning down T_d -MoTe₂ to a thickness comparable to the screening length [32, 33]. Figure 3(a) displays the gate dependence of T_c obtained from the bilayer sample. Here the gate voltage (V_g) is applied through a h-BN (34 nm in thickness) as a gate insulator. T_c is successfully modulated by V_g , and at $V_g = 8$ V it is larger by around 20 % compared with at $V_g = -8$ V. In addition to the variation of T_c , the MCA signals are also largely modulated by V_g (Fig. 3(b)). Figure 3(c) plots γ as a function of V_g . Here, γ varies with V_g , and γ at $V_g = -8$ V is almost three times larger than at $V_g = 8$ V. Note that this large variation is enabled by modulation of not only $R_{2\omega}$, but also R_ω and B .

The gate voltage can modulate some parameters relevant to superconductivity, such as T_c , B_{c2} , the magnetic penetration length λ and the coherence length ξ . Interestingly, we found that superconductivity becomes more robust as the gate voltage is made more positive. This means that B_{c2} becomes larger and ξ smaller for more positive V_g . This trend is counterintuitive when we consider the variation in $R_{2\omega}$ with V_g , because a larger B_{c2} provides larger U_0 , and a smaller ξ should be more advantageous for the ratchet-like motion. By contrast, λ , which quantifies the scale for the vortex-vortex interaction, increases as V_g decreases, concomitantly with the decline in superconductivity. Since the importance of

the vortex-vortex interaction for the ratchet-like motion has already been discussed in the context of the artificial ratchet potentials [29, 34], it may also play a role in intrinsic ratchet potentials in noncentrosymmetric superconductors. Although further theoretical studies are required to fully understand our experimental data, the demonstration of gate control of nonreciprocal transport illustrates the rich functionality of superconducting nonreciprocal devices for future applications and also provides key insights into exploring detailed mechanisms behind the ratchet-like motion of magnetic vortices.

In conclusion, we have shown giant superconducting nonreciprocal transport (MCA) in thin samples of the noncentrosymmetric superconductor T_d -MoTe₂. We obtain $3.1 \times 10^6 \text{ T}^{-1} \text{ A}^{-1}$ at 230 mK, one of the largest values of γ recorded so far. The temperature dependence of γ supports the ratchet-like motion of magnetic vortices

as the origin of the nonreciprocal transport. The giant nonreciprocal signal is likely due to the reduced symmetry of the crystal structure of T_d -MoTe₂. We have also demonstrated gate modulation of the MCA in the superconducting state. In bilayer T_d -MoTe₂, we obtain a threefold modulation of γ using a typical solid gate. Simultaneous demonstration of the gigantic MCA and its gate modulation in the superconducting state reveals that T_d -MoTe₂ is a promising candidate for realizing an electrically-tunable efficient superconducting rectification devices.

We gratefully acknowledge M. Imai, S. Sasaki, H. Murofushi and S. Wang for their support in the experiments. This project is financially supported in part by the JPSJ KAKENHI (grant no. 21H01022, 21H04652, 21K18181, 21H05236, 20H00354 and 19H05790).

-
- [1] Y. Tokura and N. Nagaosa, Nonreciprocal responses from non-centrosymmetric quantum materials, *Nature Communications* **9**, 3740 (2018).
- [2] T. Ideue, K. Hamamoto, S. Koshikawa, M. Ezawa, S. Shimizu, Y. Kaneko, Y. Tokura, N. Nagaosa, and Y. Iwasa, Bulk rectification effect in a polar semiconductor, *Nature Physics* **13**, 578 (2017).
- [3] H. F. Legg, M. Rossler, F. Munning, D. Fan, O. Breunig, A. Bliesener, G. Lippertz, A. Uday, A. A. Taskin, D. Loss, J. Klinovaja, and Y. Ando, Giant magnetochiral anisotropy from quantum-confined surface states of topological insulator nanowires, *Nature Nanotechnology* **17**, 696 (2022).
- [4] J. E. Villegas, S. Savel'ev, F. Nori, E. M. Gonzalez, J. V. Anguita, R. García, and J. L. Vicent, A superconducting reversible rectifier that controls the motion of magnetic flux quanta, *Science* **302**, 1188 (2003).
- [5] C.-S. Lee, B. Jankó, I. Derényi, and A.-L. Barabási, Reducing vortex density in superconductors using the 'ratchet effect', *Nature* **400**, 337 (1999).
- [6] C. C. de Souza Silva, J. Van de Vondel, B. Y. Zhu, M. Morelle, and V. V. Moshchalkov, Vortex ratchet effects in films with a periodic array of antidots, *Phys. Rev. B* **73**, 014507 (2006).
- [7] J. E. Villegas, E. M. Gonzalez, M. I. Montero, I. K. Schuller, and J. L. Vicent, Directional vortex motion guided by artificially induced mesoscopic potentials, *Phys. Rev. B* **68**, 224504 (2003).
- [8] B. Y. Zhu, L. V. Look, V. V. Moshchalkov, B. R. Zhao, and Z. X. Zhao, Vortex dynamics in regular arrays of asymmetric pinning centers, *Phys. Rev. B* **64**, 012504 (2001).
- [9] J. E. Villegas, E. M. Gonzalez, M. P. Gonzalez, J. V. Anguita, and J. L. Vicent, Experimental ratchet effect in superconducting films with periodic arrays of asymmetric potentials, *Phys. Rev. B* **71**, 024519 (2005).
- [10] S. Hoshino, R. Wakatsuki, K. Hamamoto, and N. Nagaosa, Nonreciprocal charge transport in two-dimensional noncentrosymmetric superconductors, *Phys. Rev. B* **98**, 054510 (2018).
- [11] Y. M. Itahashi, Y. Saito, T. Ideue, T. Nojima, and Y. Iwasa, Quantum and classical ratchet motions of vortices in a two-dimensional trigonal superconductor, *Phys. Rev. Research* **2**, 023127 (2020).
- [12] T. Ideue, S. Koshikawa, H. Namiki, T. Sasagawa, and Y. Iwasa, Giant nonreciprocal magnetotransport in bulk trigonal superconductor PbTase₂, *Phys. Rev. Research* **2**, 042046 (2020).
- [13] A. Daido, Y. Ikeda, and Y. Yanase, Intrinsic superconducting diode effect, *Phys. Rev. Lett.* **128**, 037001 (2022).
- [14] R. Wakatsuki and N. Nagaosa, Nonreciprocal current in noncentrosymmetric Rashba superconductors, *Phys. Rev. Lett.* **121**, 026601 (2018).
- [15] R. Wakatsuki, Y. Saito, S. Hoshino, Y. M. Itahashi, T. Ideue, M. Ezawa, Y. Iwasa, and N. Nagaosa, Nonreciprocal charge transport in noncentrosymmetric superconductors, *Science Advances* **3**, e1602390 (2017).
- [16] E. Zhang, X. Xu, Y.-C. Zou, L. Ai, X. Dong, C. Huang, P. Leng, S. Liu, Y. Zhang, Z. Jia, X. Peng, M. Zhao, Y. Yang, Z. Li, H. Guo, S. J. Haigh, N. Nagaosa, J. Shen, and F. Xiu, Nonreciprocal superconducting NbSe₂ antenna, *Nature Communications* **11**, 5634 (2020).
- [17] Y. M. Itahashi, T. Ideue, S. Hoshino, C. Goto, H. Namiki, T. Sasagawa, and Y. Iwasa, Giant second harmonic transport under time-reversal symmetry in a trigonal superconductor, *Nature Communications* **13**, 1659 (2022).
- [18] P. J. Zomer, M. H. D. Guimaraes, J. C. Brant, N. Tombros, and B. J. van Wees, Fast pick up technique for high quality heterostructures of bilayer graphene and hexagonal boron nitride, *Applied Physics Letters* **105**, 013101 (2014).
- [19] Supplemental material, .
- [20] G. L. J. A. Rikken, J. Folling, and P. Wyder, Electrical magnetochiral anisotropy, *Phys. Rev. Lett.* **87**, 236602 (2001).
- [21] Y. Qi, P. G. Naumov, M. N. Ali, C. R. Rajamathi, W. Schnelle, O. Barkalov, M. Hanfland, S.-C. Wu, C. Shekhar, Y. Sun, V. Suss, M. Schmidt, U. Schwarz, E. Pippel, P. Werner, R. Hillebrand, T. Forster, E. Kampert, S. Parkin, R. J. Cava, C. Felser, B. Yan, and S. A. Medvedev, Superconductivity in Weyl semimetal candi-

- date MoTe₂, *Nature Communications* **7**, 11038 (2016).
- [22] D. A. Rhodes, A. Jindal, N. F. Q. Yuan, Y. Jung, A. Antony, H. Wang, B. Kim, Y.-c. Chiu, T. Taniguchi, K. Watanabe, K. Barmak, L. Balicas, C. R. Dean, X. Qian, L. Fu, A. N. Pasupathy, and J. Hone, Enhanced superconductivity in monolayer T_d-MoTe₂, *Nano Letters* **21**, 2505 (2021).
- [23] Y. Gan, C.-W. Cho, A. Li, J. Lyu, X. Du, J.-S. Wen, and L.-Y. Zhang, Giant enhancement of superconductivity in few layers MoTe₂, *Chinese Physics B* **28**, 117401 (2019).
- [24] Y. M. Itahashi, T. Ideue, Y. Saito, S. Shimizu, T. Ouchi, T. Nojima, and Y. Iwasa, Nonreciprocal transport in gate-induced polar superconductor SrTiO₃, *Science Advances* **6**, eaay9120 (2020).
- [25] M. Tinkham, *Introduction to Superconductivity: 2nd Ed.* (Dover Publications, 2004).
- [26] W.-K. Kwok, U. Welp, A. Glatz, A. E. Koshelev, K. J. Kihlstrom, and G. W. Crabtree, Vortices in high-performance high-temperature superconductors, *Reports on Progress in Physics* **79**, 116501 (2016).
- [27] A. Fente, W. R. Meier, T. Kong, V. G. Kogan, S. L. Bud'ko, P. C. Canfield, I. Guillamón, and H. Suderow, Influence of multiband sign-changing superconductivity on vortex cores and vortex pinning in stoichiometric high-*T_c* CaKFe₄As₄, *Phys. Rev. B* **97**, 134501 (2018).
- [28] K. Hamamoto, T. Park, H. Ishizuka, and N. Nagaosa, Scaling theory of a quantum ratchet, *Phys. Rev. B* **99**, 064307 (2019).
- [29] A. Palau, C. Monton, V. Rouco, X. Obradors, and T. Puig, Guided vortex motion in YBa₂Cu₃O₇ thin films with collective ratchet pinning potentials, *Phys. Rev. B* **85**, 012502 (2012).
- [30] D. J. Morgan and J. B. Ketterson, Asymmetric flux pinning in a regular array of magnetic dipoles, *Phys. Rev. Lett.* **80**, 3614 (1998).
- [31] D. Choe, M.-J. Jin, S.-I. Kim, H.-J. Choi, J. Jo, I. Oh, J. Park, H. Jin, H. C. Koo, B.-C. Min, S. Hong, H.-W. Lee, S.-H. Baek, and J.-W. Yoo, Gate-tunable giant nonreciprocal charge transport in noncentrosymmetric oxide interfaces, *Nature Communications* **10**, 4510 (2019).
- [32] Q. Ma, S.-Y. Xu, H. Shen, D. MacNeill, V. Fatemi, T.-R. Chang, A. M. Mier Valdivia, S. Wu, Z. Du, C.-H. Hsu, S. Fang, Q. D. Gibson, K. Watanabe, T. Taniguchi, R. J. Cava, E. Kaxiras, H.-Z. Lu, H. Lin, L. Fu, N. Gedik, and P. Jarillo-Herrero, Observation of the nonlinear Hall effect under time-reversal-symmetric conditions, *Nature* **565**, 337 (2019).
- [33] Z. Fei, W. Zhao, T. A. Palomaki, B. Sun, M. K. Miller, Z. Zhao, J. Yan, X. Xu, and D. H. Cobden, Ferroelectric switching of a two-dimensional metal, *Nature* **560**, 336 (2018).
- [34] C. J. Olson, C. Reichhardt, B. Jankó, and F. Nori, Collective interaction-driven ratchet for transporting flux quanta, *Phys. Rev. Lett.* **87**, 177002 (2001).

